Visible quantum cutting in $GdF_3:Eu^{3+}$ nanocrystals via downconversion

2006 Nanotechnology 17 1642

(http://iopscience.iop.org/0957-4484/17/6/017)

INSTITUTE OF PHYSICS PUBLISHING NANOTECHNOLOGY
Nanotechnology **17** (2006) 1642–1645 doi:10.1088/0957-4484/17/6/017

Visible quantum cutting in $GdF_3:Eu^{3+}$ nanocrystals via downconversion

Ruinian Hua[1,3], Jinghua Niu[2], Baojiu Chen[2], Mingtao Li[2], Tianzhi Yu[2] and Wenlian Li[2,3]

[1] College of Life Science, Dalian Nationalities University, Dalian 116600, People's Republic of China
[2] Key Laboratory of Excited State Process, Changchun Institute of Optics, Fine Mechanics and Physics, Chinese Academy of Sciences, Changchun 130033, People's Republic of China

E-mail: rnhua@dlnu.edu.cn

Received 24 October 2005, in final form 27 December 2005
Published 27 February 2006
Online at stacks.iop.org/Nano/17/1642

Abstract
$GdF_3:Eu^{3+}$ nanocrystals (NCs) and nanorods were synthesized by a microemulsion-mediated hydrothermal process. The structure, shape and particle size were characterized by means of x-ray diffraction (XRD) and transmission electron microscopy (TEM). The vacuum ultraviolet (VUV) spectrum of $GdF_3:Eu^{3+}$ NCs shows that the Gd^{3+} ion can absorb one VUV photon excited in the ^6G_J levels and relaxes through two-step energy transfer to Eu^{3+}, yielding two visible photons at room temperature. The visible quantum efficiency of $GdF_3:Eu^{3+}$ NCs was calculated to be close to 170% by the peak intensity ratio of correlative transition emission under VUV excitation at 160 nm.

1. Introduction

In the past decades the development of phosphors for excitation in the vacuum ultraviolet (VUV) has become an important new topic in the field of luminescent material research [1–6]. VUV phosphors are required for application in mercury-free fluorescent tubes and in plasma display panels. The VUV phosphors used in mercury fluorescent tubes have quantum efficiencies close to 100%. Therefore, to make a noble gas discharge fluorescent tube a competitive phosphor with a quantum efficiency greater than 100% is required, i.e. more than one visible photon should be obtained per absorbed VUV photon, a so-called quantum cutter [7]. Wegh *et al* [8, 9] presented a quantum cutter concept based on the Gd^{3+}–Eu^{3+} couple in $LiGdF_4:Eu^{3+}$. The internal quantum yield was determined to be approximately 200% by comparing the intensity ratio under 273 nm excitation ($^8S_{7/2}$–^6I_J) with that under 202 nm excitation into the higher ^6G_J level of Gd^{3+}. Similar work based on Gd^{3+}–Eu^{3+} couples has also been reported by the Feldmann group [10] and the Lin group [11]. Feldmann *et al* determined the external quantum efficiency to be 32%, which was obtained for $^8S_{7/2}$–^6G_J excitation at 202 nm (the absolute light output and external quantum efficiency were derived by using Y_2O_3:Eu as a reference) [10]. Lin *et al* determined the visible quantum efficiency to be 160%, which was obtained for $^8S_{7/2}$–^6G_J excitation at 194 nm (non-radiative losses due to UV emission from Gd^{3+} are negligible) [11]. In the $GdF_3:Eu^{3+}$ single-crystal system [9], $4f^65d$–$4f^7$ emission of Eu^{2+} ions is due to the reducing atmosphere during the preparation of the sample in a carbon crucible, and the relative increase of $^5D_0$, $^5D_{1,2,3}$ emission is much larger for $GdF_3:Eu^{3+}$ than for $LiGdF_4:Eu^{3+}$. Because energy transfer from Gd^{3+} to Eu^{3+} in GdF_3 is not as efficient as in $LiGdF_4$, in the meanwhile the presence of the Gd^{3+} $^6G_J \rightarrow {}^6P_J$ and $Eu^2 + 4f^65d \rightarrow 4f^7$ emissions in the spectra makes calculation of the efficiency of the two-step energy transfer process more complicated than that for $LiGdF_4:Eu^{3+}$. So the efficiency of the cross-relaxation step was calculated, by the same method as for $LiGdF_4:Eu^{3+}$, to lie between 80% and 100% [9]. Berkowitz *et al* [12] measured the absolute vacuum ultraviolet-to-visible conversion, or quantum efficiency of a number of phosphor systems (Zn_2SiO_4:Mn, Y_2O_3:Eu, YVO_4:Eu, ZnS:M (M = Cu, Ag, Ag + Cu, and Cu + Al), ZnO:Zn and $GdPO_4$:Re (Re = Eu, Tb, and Ce + Tb)) for VUV excitation energies from 5 to 25 eV. Their results demonstrate the need to minimize loss mechanisms such as colour centres, trapping levels and surface defects. These loss mechanisms can easily dominate the photoluminescent process, preventing

[3] Authors to whom any correspondence should be addressed.

a phosphor which exhibits multiple photon emission processes from achieving a quantum efficiency greater than 1.

Rare earth (or metal) fluorides are normally synthesized by a traditional high-temperature solid state reaction, which requires a complicated set-up under an atmosphere of F_2 or HF mixed with an inert carrier gas to avoid possible contamination from oxygen [13]. Recently, mild hydrothermal [14] and solvothermal reactions [15, 16] have been developed to synthesize fluorides. The products based on these procedures usually exhibit relatively large and variable grain sizes. Since Bender *et al* [17] synthesized neodymium-doped barium fluoride nanoparticles via a reverse micelles technique, reverse microemulsions have been successfully used for the synthesis of CeF_3 [18], BaF_2:Ce [19], BaF_2:Er [20] nanoparticles and BaF_2 nanowires [21]. Complex fluorides such as $LiBaF_3$ [22] and KMF_3 (M = Zn and Cd) [23] nanocrystals (NCs) have also been prepared by a microemulsion process and mild solvothermal process, respectively. So far, there have been no reports of preparation of GdF_3 NCs. Here we report a microemulsion-mediated hydrothermal process for preparing GdF_3:Eu^{3+} NCs and nanorods using $GdCl_3{\cdot}6H_2O$, $EuCl_3{\cdot}6H_2O$ and NH_4F (or HF) as precursors. Their structure, shape and particle size were characterized by means of XRD and TEM. A visible quantum efficiency of GdF_3:Eu^{3+} NCs was also obtained for $^8S_{7/2}$–^6G_J excitation at 160 nm.

2. Experimental details

All the reagents used in this study were analytically pure except for spectrographically pure Gd_2O_3 and Eu_2O_3. $GdCl_3{\cdot}6H_2O$ and $EuCl_3{\cdot}6H_2O$ were prepared by dissolving Gd_2O_3 and Eu_2O_3 in hydrochloric acid and then recrystallizing five times. Europium-doped GdF_3 NCs and nanorods were prepared from the quaternary reverse micelles of cetyltrimethylammonium bromide (CTAB), cyclohexane, *n*-pentanol and water. In a typical synthesis, two identical solutions were prepared by dissolving CTAB (2.0 g) in 31 ml of cyclohexane and 2.0 ml of *n*-pentanol. The mixing solution was stirred for 30 min until it became transparent. Next, 2 ml of $GdCl_3$ and $EuCl_3$ aqueous solution (containing 1×10^{-3} mol $GdCl_3{\cdot}6H_2O$ and 5×10^{-6} mol $EuCl_3{\cdot}6H_2O$, the Eu^{3+} concentration was 0.5 mol% referred to Gd^{3+}) and 2 ml of 6.0% HF aqueous solution (or 2 ml of 1.5 mol l^{-1} NH_4F aqueous solution) were added to the respective solutions. After substantial stirring, the two optically transparent microemulsion solutions were mixed and stirred for another 30 min. The resulting microemulsion solution was then transferred into a 100 ml stainless Teflon-lined autoclave and heated at 150 °C for 10 h. The resulting suspension was allowed to cool to room temperature. After 12 h of ageing, the final products were collected and washed several times with methanol and distilled water. Finally, the GdF_3:Eu^{3+} (0.5 mol%) NCs were obtained after the samples were centrifuged and dried in a vacuum at room temperature.

The phase purity of GdF_3:Eu^{3+} NCs was characterized by a Rigaku D/max-II B x-ray powder diffractometer using Cu Kα_1 radiation (λ = 0.1541 nm). The step-scan covered the angular range from 20 to 60 in steps of 0.02. The morphology of the products was examined on a field emission scanning electron microscope (FESEM, XL30 ESEM FEG) and a JEM-2000FX transmission electron microscope (TEM) with accelerating voltage of 160 kV. The VUV spectra of GdF_3:Eu^{3+} NCs was obtained with a VUV spectrofluorometer with a deuterium lamp as the light source. Photoluminescent spectra were measured using a Hitachi F-4500 fluorescence spectrometer.

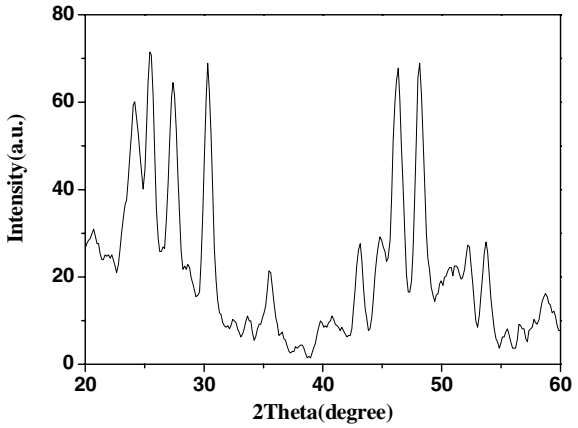

Figure 1. XRD pattern of GdF_3:Eu^{3+} (0.5 mol%) NCs.

3. Results and discussion

Figure 1 shows the XRD pattern of the Eu-doped GdF_3 NCs a dopant level of 0.5 mol%. It can be readily indexed to an orthorhombic phase (space group *Pnma*) with a lattice constant a = 6.575 Å, b = 4.986 Å and c = 4.394 Å, which is in agreement with the standard values for the bulk GdF_3 (JCPDS 49-1804). No other peaks or impurities are detected. Therefore, XRD confirmed the phase purity of the GdF_3:Eu^{3+} (0.5 mol%) NCs obtained from the microemulsion-mediated hydrothermal process. According to the Scherrer equation, the size of the GdF_3:Eu^{3+} particles was estimated to be about 20 nm.

The FESEM and TEM images of the products shown in figure 2 indicated that GdF_3:Eu^{3+} are a mixture of NCs and a small number of nanorods. The size of the GdF_3:Eu^{3+} NCs is about 18 nm. The GdF_3:Eu^{3+} nanorods are 60–200 nm in length and 18–20 nm in diameter, in agreement with the XRD result. The similar sizes and shapes of products were obtained by using different precipitators such as HF aqueous solution and NH_4F solution. A water-in-oil (W/O) microemulsion is a transparent and isotropic liquid medium with nanosized water pools dispersed in a continuous phase and stabilized by surfactant and cosurfactant molecules at the water/oil interface. These water pools offer ideal microreactors for the formation of GdF_3:Eu^{3+} nanocrystals under hydrothermal conditions. The appearance of some of the nanorods in the samples indicated that hydrothermal conditions and a medium surfactant concentration (0.06 mol l^{-1} < M_{CTAB} < 1.5 mol l^{-1}) may affect the micellar sizes (nanosized water pools) and shapes [21].

Excitation spectra of the $^5D_0$–$^7F_2$ emission of Eu^{3+} (614 nm) at room temperature (298 K) is shown in figure 3. The excitation spectra of the $^5D_0$ emission indicated that the two sharp peaks, located at 205 and 273 nm correspond to excitation into the Gd^{3+} ^6G_J ($^8S_{7/2}$–^6G_J) and ^6I_J ($^8S_{7/2}$–^6I_J)

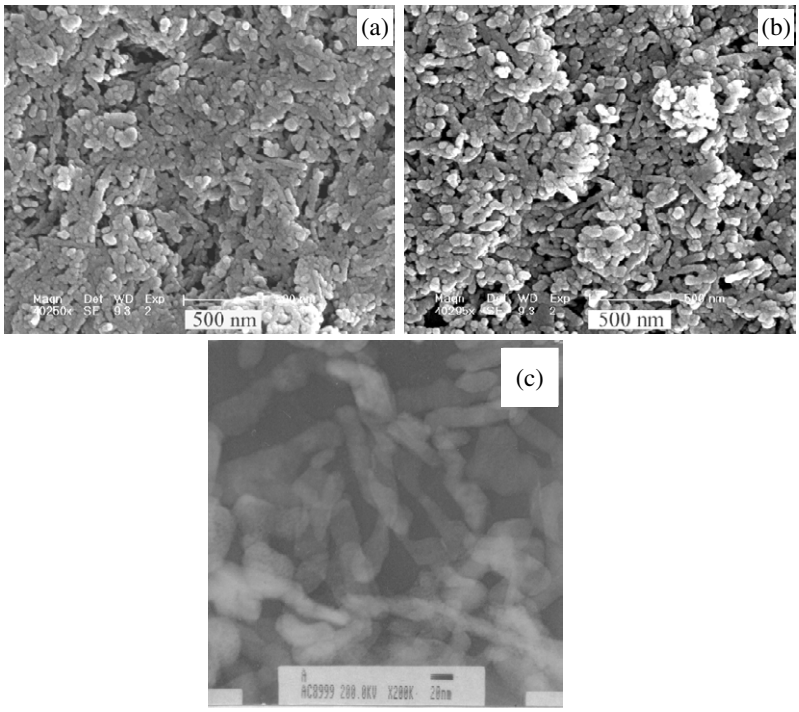

Figure 2. FESEM images and TEM micrograph of GdF_3:Eu^{3+} (0.5 mol%) NCs. (a) FESEM image of NCs using $GdCl_3{\cdot}6H_2O$, $EuCl_3{\cdot}6H_2O$ and HF as precursors. (b) FESEM image using $GdCl_3{\cdot}6H_2O$, $EuCl_3{\cdot}6H_2O$ and NH_4F as precursors. (c) TEM micrograph by using $GdCl_3{\cdot}6H_2O$, $EuCl_3{\cdot}6H_2O$ and HF as precursors.

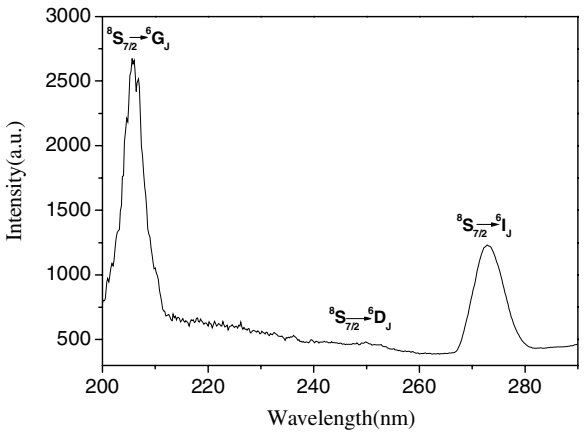

Figure 3. Excitation spectra of GdF_3:Eu^{3+} (0.5 mol%) NCs monitored at 614 nm ($^5D_0$–$^7F_2$ emission of Eu^{3+})

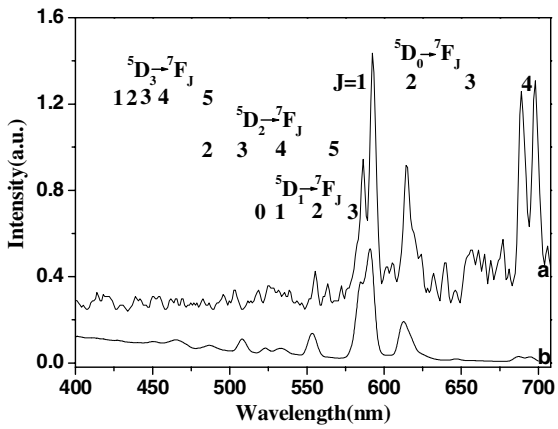

Figure 4. Emission spectra of GdF_3:Eu^{3+} (0.5 mol%) upon (a) $^8S_{7/2}$–^6G_J excitation on Gd^{3+} (160 nm) at 300 K and (b) $^8S_{7/2}$–^6I_J excitation on Gd^{3+} (273 nm) at 300 K.

levels, respectively. This confirms the occurrence of two-step energy transfer from the ^6G_J level of Gd^{3+} to Eu^{3+}. In the Gd^{3+}–Eu^{3+} couple, the first step of the energy transfer occurs by cross relaxation between the ^6G_J state in Gd^{3+} and the ^7F_J ground state in Eu^{3+}, resulting in the $^5D_0$ excited state in Eu^{3+} and the $6P_J$ state in Gd^{3+}. In the second step, the Gd^{3+} ion in the ^6P_J state transfers the remaining excitation energy to a second Eu^{3+} ion, which is followed by fast relaxation to the ^5D_J states. Both steps result in the emission of a visible photon due to the ^5D_J–^7F_J transitions on Eu^{3+} [8, 9]. In figure 3, the Gd^{3+} $^8S_{7/2}$–^6D_J transition is hardly observed relative to the $^8S_{7/2}$–^6G_J and $^8S_{7/2}$–^6I_J. The line intensity of the $^8S_{7/2}$–^6G_J excitation appears to be about double that of the $^8S_{7/2}$–^6I_J line.

Figure 4 shows the emission spectra of GdF_3:Eu^{3+} (0.5 mol%) NCs at room temperature upon excitation in the ^6G_J (160 nm) levels and ^6I_J (273 nm) levels, respectively. The $^5D_0$, $^5D_1$, $^5D_2$ and $^5D_3$–^7F_J emissions due to transitions on the Eu^{3+} ion are shown. From figure 4, the visible quantum cutting by two-step energy transfer occurs in GdF_3:Eu^{3+} NCs because the $^5D_0$ emission intensity increases relative to $^5D_{1,2,3}$ emission upon ^6G_J excitation compared with ^6I_J excitation. Several emission lines which cannot be assigned to ^5D_J–^7F_J transitions are observed in the region between 410 and 570 nm. From the emission spectrum upon excitation in Gd^{3+} ^6G_J (figure 4(a) curve) and ^6I_J (figure 4(b) curve), the $^5D_0/^5D_{1,2,3}$

emission intensity ratios are about 4.3 and 2.1 according to the quantum efficiency equation of Wegh *et al* [8]:

$$\frac{P_{CR}}{P_{CR}+P_{DT}} = \frac{R(^5D_0/^5D_{1,2,3})_{^6G_J} - R(^5D_0/^5D_{1,2,3})_{^6I_J}}{R(^5D_0/^5D_{1,2,3})_{^6I_J}+1}.$$

In this way, a large part of the VUV excitation energy of Gd^{3+} may be lost through non-radiative relaxation (zero photon emission), particularly in GdF_3:Eu^{3+} nanocrystals. Non-radiative losses at defects and impurities can lower the quantum efficiency. A visible quantum efficiency of about 170% for GdF_3:Eu^{3+} (0.5 mol%) NCs upon excitation in ^6G_J can be obtained if non-radiative losses can be prevented (for example, losses due to energy migration and energy transfer to non-radiative quenching centres in the lattice). In Wegh's report, experience with lanthanide phosphors has shown that non-radiative losses can be low if the synthesis procedure is optimized [8]. Thus, in an optimized GdF_3:Eu^{3+} NCs phosphor, a visible quantum efficiency of about 170% may be possible if non-radiative losses due to UV emission from Gd^{3+} are negligible. This value is approximately consistent with Wegh's report for the GdF_3:Eu^{3+} single-crystal system [9]. In this research we have not been able to determine absolute quantum efficiencies of phosphors under VUV excitation, however Feldmann *et al* did some excellent work [10]. The results reported here, however, show that the two-step energy transfer process occurs with a higher efficiency.

4. Conclusion

In summary, europium-doped GdF_3 nanocrystals have been successfully prepared for the first time using the microemulsion-mediated hydrothermal process. The final products are NCs of 18 nm in size and a few nanorods of 60–200 nm in length and 18–20 nm in diameter. Excitation spectra of the $^5D_0$–$^7F_2$ emission of Eu^{3+} (614 nm) and emission spectra at room temperature (298 K) confirm the occurrence of two-step energy transfer from the ^6G_J level of Gd^{3+} to Eu^{3+}. The visible quantum efficiency upon excitation in ^6G_J is close to 170% for GdF_3:Eu^{3+} (0.5 mol%) NCs (if non-radiative losses due to UV emission from Gd^{3+} are negligible). Future research on quantum cutting phosphors based on fluoride nanocrystals should concentrate on improvement of the quantum efficiency. Meanwhile, studies of the possibility of synthesizing other rare earth ion-doped fluoride nanostructures using a similar method are under way.

Acknowledgments

This work was supported by the Postdoctoral Fund of Dalian Nationalities University (20056110) and the Young People Innovative Foundation of Changchun Institute of Optics, Fine Mechanics and Physics, Chinese Academy of Sciences (Q03M18Z).

References

[1] Sommerdijk J L, Bril A and De Jager A W 1974 *J. Lumin.* **8** 341
[2] Sommerdijk J L, Bril A and De Jager A W 1974 *J. Lumin.* **9** 288
[3] Piper W W, DeLuca J A and Ham F S 1974 *J. Lumin.* **8** 344
[4] Pappalardo R 1976 *J. Lumin.* **14** 159
[5] Srivastava A M and Beers W W 1997 *J. Lumin.* **71** 285
[6] Joubert M F, Linares C, Jacquier B, Cassanho A and Jenssen H P 1992 *J. Lumin.* **51** 175
[7] Wegh R T, Donker H, Meijerink A, Lamminmaki R J and Holsa J 1997 *Phys. Rev.* B **56** 13841
[8] Wegh R T, Donker H, Oskam K D and Meijerink A 1999 *Science* **283** 663
[9] Wegh R T, Donker H, Oskam K D and Meijerink A 1999 *J. Lumin.* **82** 93
[10] Feldmann C, Justel T, Ronda C R and Wiechert D U 2001 *J. Lumin.* **92** 245
[11] You F T, Wang Y X, Lin J H and Tao Y 2001 *Chin. J. Inorg. Chem.* **17** 27
[12] Berkowitz J K and Olsen J A 1991 *J. Lumin* **50** 111
[13] Su H, Jia Z and Shi C 2002 *Chem. Mater.* **14** 310
[14] Zhao C, Feng S, Chao Z, Shi C, Xu R and Ni J 1996 *Chem. Commun.* 1641
[15] Hua R, Jia Z, Xie D and Shi C 2002 *Chem. Lett.* **31** 538
[16] Hua R, Lei B, Xie D and Shi C 2003 *J. Solid State Chem.* **175** 284
[17] Bender C M, Burlitch J M, Barber D and Pollock C 2000 *Chem. Mater.* **12** 1969
[18] Qiu S, Dong J and Chen G 2000 *Powder Technol.* **113** 9
[19] Hua R, Zang C, Shao C, Xie D and Shi C 2003 *Nanotechnology* **6** 588
[20] Lian H, Liu J, Ye Z and Shi C 2004 *Chem. Phys. Lett.* **386** 291
[21] Cao M, Hu C and Wang E 2003 *J. Am. Chem. Soc.* **125** 11196
[22] Hua R, Xie D and Shi C 2004 *Chin. Chem. Lett.* **15** 238
[23] Huang B, Hong J, Chen X, Yu Z and You X 2005 *Mater. Lett.* **59** 430